NRIAG JOURNAL OF ASTRONOMY AND GEOPHYSICS
2020, VOL. 9, NO. 1, 52–62
https://doi.org/10.1080/20909977.2020.1711696

Taylor & Francis
Taylor & Francis Group

OPEN ACCESS Check for updates

Sequoia reservoir evaluation through conventional petrophysical analysis in Eastern Mediterranean, Nile Delta, Egypt

Hassan M. El Shayeb[a], Gouda I. Abdel-Gawad[b], Ahmed Z. Noah[c], Mohamed M. Abuelhasan[a] and Mohamed A. Ataallah[d]

[a]Department of Geology, Faculty of Science, University of Menoufia, Shebeen El-Kom, Egypt; [b]Department of Geology, Faculty of Science, University of Beni-Suef, Beni-Suef, Egypt; [c]Department of Exploration, Egyptian Petroleum Research Institute (EPRI), Cairo, Egypt; [d]Department of Petroleum geology and Natural Gas, Faculty of Earth Sciences, University of Beni-Suef, Beni-Suef, Egypt

ABSTRACT
The Sequoia Field, in West Delta Deep Marine concession, represents deep marine slope channels in Nile Delta of Egypt. The main hydrocarbon bearing formation is the Late Pliocene El Wastani Formation. Sequoia Channel of the El Wastani Formation are considered as the main reservoirs of Sequoia Field. Well log data analysis, of five wells were accomplished using computer software programs (e.g. Interactive petrophysics (I.P.) Software was used in petrophysical evaluation for Petrophysical analysis, in terms of determining the effective porosity, shale volume, and reservoir fluid saturation of Sequoia Channel of El Wastani Formation, is the primary aim of this study in order to achieve better determination of the reservoir quality in Sequoia Field. We found that Sequoia Channel of El Wastani Formation is having high storage capacity properties permit them of bearing a good amount of hydrocarbon fluids in the Sequoia Field. It was found that effective porosity ranges between 19% and 29%, shale content ranges between 10% and 28%, the water saturation ranges between 15% and 40%. It is clear that the facies effect is the main factor that is controlling the distribution of the petrophysical properties.

ARTICLE HISTORY
Received 18 October 2019
Revised 10 December 2019
Accepted 27 December 2019

KEYWORDS
Petrophysical; Sequoia field; Eastern Mediterranean; Nile Delta; Egypt

1. Introduction

The Sequoia field is in the West Delta Deep Marine (WDDM) concession Figure (1) was attained by BG Group and its partner Edison Gas in 1995 (Alami 2006) and (Mohamed et al. 2015). The WDDM concession lies 50–100 km offshore and is covering 6150 km^2 of northwest margin of Nile Delta cone (Samuel et al. 2003). The Sequoia field is a Pliocene gas field in the WDDM located about 90 km north Nile Delta shoreline and is in water depths of 150–750 m. WDDM concession in the Mediterranean Sea comprises 19 gas fields, of which 12 fields (Scarab, Saffron, Simian, Sienna, Sapphire, Serpent, Saurus, Sequoia, SimSat-P2, Sapsat-1, Sapsat-2 and Swan) are in production. The fields are located at water depths ranging from 700 m to 850 m and approximately 90 km to120km from the shore. The operator BG Egypt won the WDDM concession in 1995. It holds a 50% interest, while the remaining 50% interest is held by Petronas, which acquired Edison International's share in 2003. Burullus Gas Company, a joint-venture (JV) of EGPC (50%), BG Egypt (25%) and Petronas (25%), carries out the operations on behalf of the WDDM partners. In 2006 Rashpetco/Burullus acquired a high-density development 3D seismic survey covering all of its discovered & producing Pliocene Gas fields in the WDDM Concession. This survey was extended slightly to cover the Rosetta Concession portion of the **Sequoia field**, thus ensuring a consistent seismic database would be available for the development work. The architecture of slope channel complexes is illustrated by (Mayall and Stewart 2000) In early 2007 a dedicated volume of seismic covering the **Sequoia field** area was processed, with parameters specifically targeting improving resolution at the Sequoia field level. The project was completed in early 2008, bringing seven additional wells into production. In phase 5 of the WDDM development, involving the installation of two gas turbine-driven compression sets, new absorption towers and associated equipment to increase production from the Scarab and Saffron facilities. And in phase 6, which involving the development of the **Sequoia field**, the field features six subsea wells, including three wells in each concession, and is interconnected to the existing facilities at WDDM. Charging of the reservoir is from the north, and the gas is a mixture of biogenic and thermogenic origin. The most significant structural element of the Sequoia field is the presence of the broadly east–northeast/west – southwest extensional fault that cuts across the WDDM concession. This extensional fault has

CONTACT Mohamed A. Ataallah mohamed_abdelwahab@esc.bsu.edu.eg Department of Petroleum geology and Natural Gas, Faculty of Earth Sciences, University of Beni- Suef, Beni-Suef, Egypt

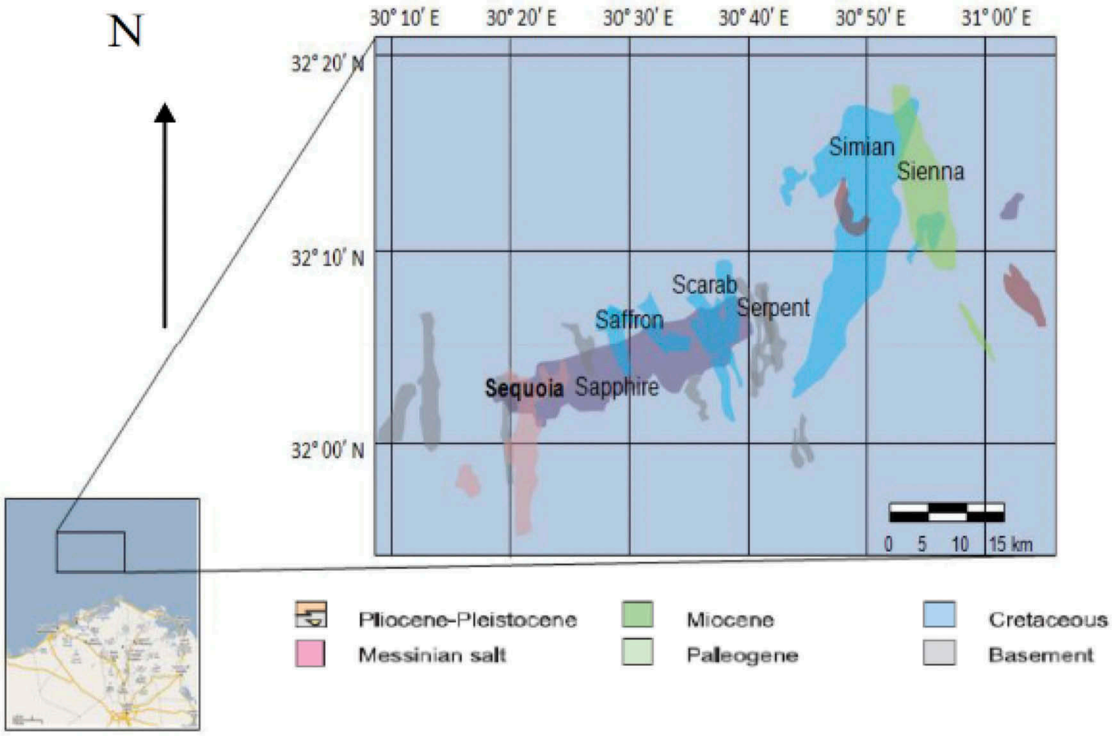

Figure 1. Location and geological map of Sequoia field.

a down-throw to the north, with a maximum displacement of 120 m form the centre of the field, reducing to less than 10 m on its eastern and western limits, the same as described by (Cross et al. 2009).

2. Geological setting

The penetrated sedimentary sequence of the Nile Delta ranges in age from Lower Miocene to Recent Figure (2) as mentioned by Samuel et al. (2003). Harms and Wray (1990) stated that the succession of the Nile Delta shows variations in both thickness and facies. The thickness increases gradually from south-to -north and abruptly towards the NE and NW. He also mentioned that sandstones with lenses of gravels are common in the south of the Nile Delta area, which grade laterally into sandstones interbedded with clays. These lateral facies changes indicate that the sources of these detrital sediments where the Eastern Desert and the Red Sea Hills. (Doherty et al. 1988) subdivided the stratigraphy of the offshore Nile Delta into three units namely;

(1) The Plio-Pleistocene Unit that marks the major out building phases of the delta and is dominated by shale. This unit includes (Bilqas, Mit Ghamr, El-Wastani and Kafr El-Sheik formations).
(2) The Miocene Unit that comprises a sandwich with two sand packages, (Abu Madi and Qawasim formations, separated by Messinian Rosetta Anhydrite Formation).
(3) The Middle-Lower Miocene Unit, which is mainly composed of shales with sand stringers and includes (Sidi Salem and Qantara (Moghra) formations).

(Younes 2001) evaluated the hydrocarbon potential in offshore Nile Delta and reported that shales in the Moghra and Sidi Salim formations reached to the peak of hydrocarbon generation at 4–6 million years. The main source rocks are believed to occur in the late Mesozoic and Oligocene to early Miocene sediments (Vandré et al. 2007). The structural setting of the WDDM area shows that it is a fault-bounded block with complex interplay among three main fault trends; the Southwest-Northeast trending Rosetta fault in the Southeast, large East-West faults in the Northeast with rotated fault blocks making the Northwestern boundary (Abdel Aal et al. 2000) and (Mayall et al. 2006). As shown on Figure 3, the Rosetta fault is the largest in the region, a major SW-NE orientated extensional to a strike-slip fault probably active during Pliocene reservoir deposition (Cross et al. 2009). Basement controlled faults, inherited from Tethyan rifting were important during the pre-Pliocene (Vandré et al. 2007). Prior to when much of the high-quality reservoir sands were deposited. On top of this, active subduction of the Northern margin of the African plate had been occurring since the Late Cretaceous along the destructive compression plate boundary of Crete and Cyprus (Vandré et al. 2007). Petrophysical analysis of Sequoia channel of El Wastani Formation is the

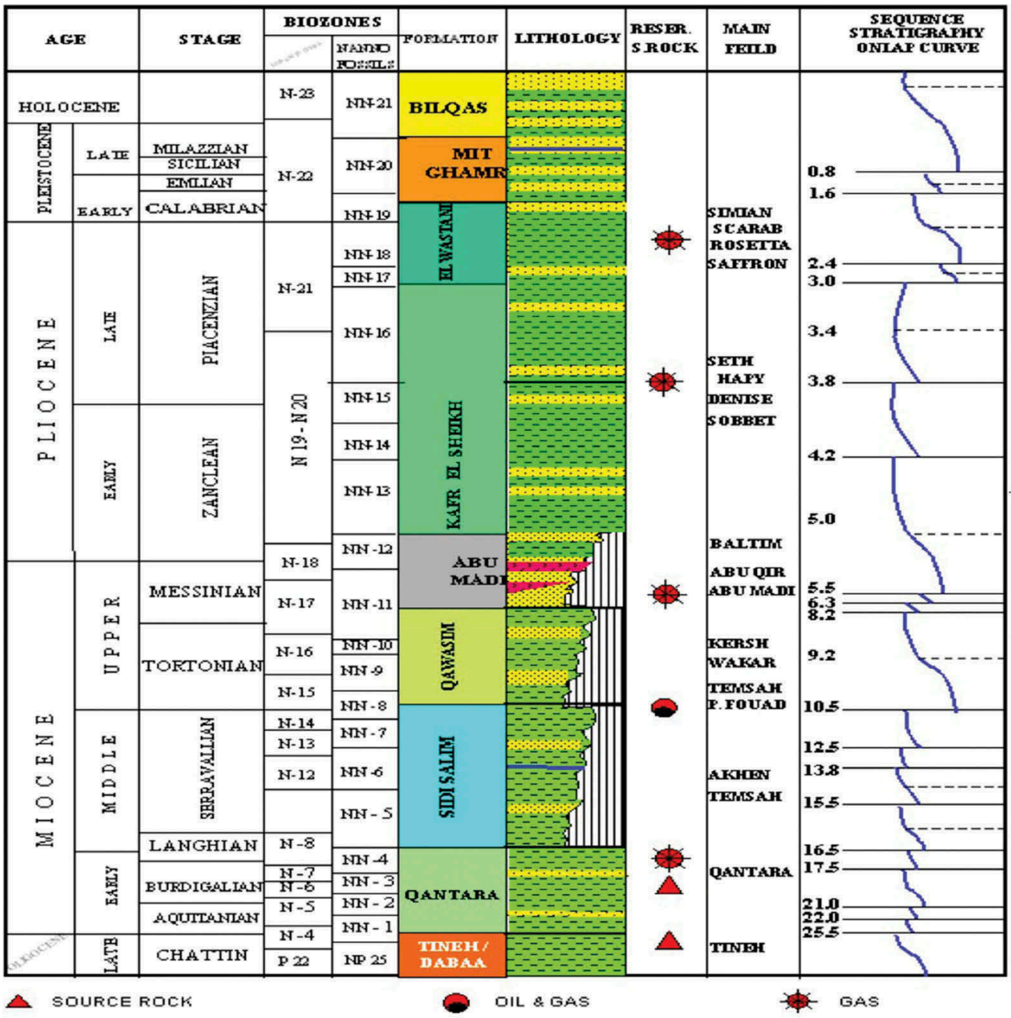

Figure 2. Generalised lithostratigraphic column of the Rosetta field in our study area (Samuel et al. 2003).

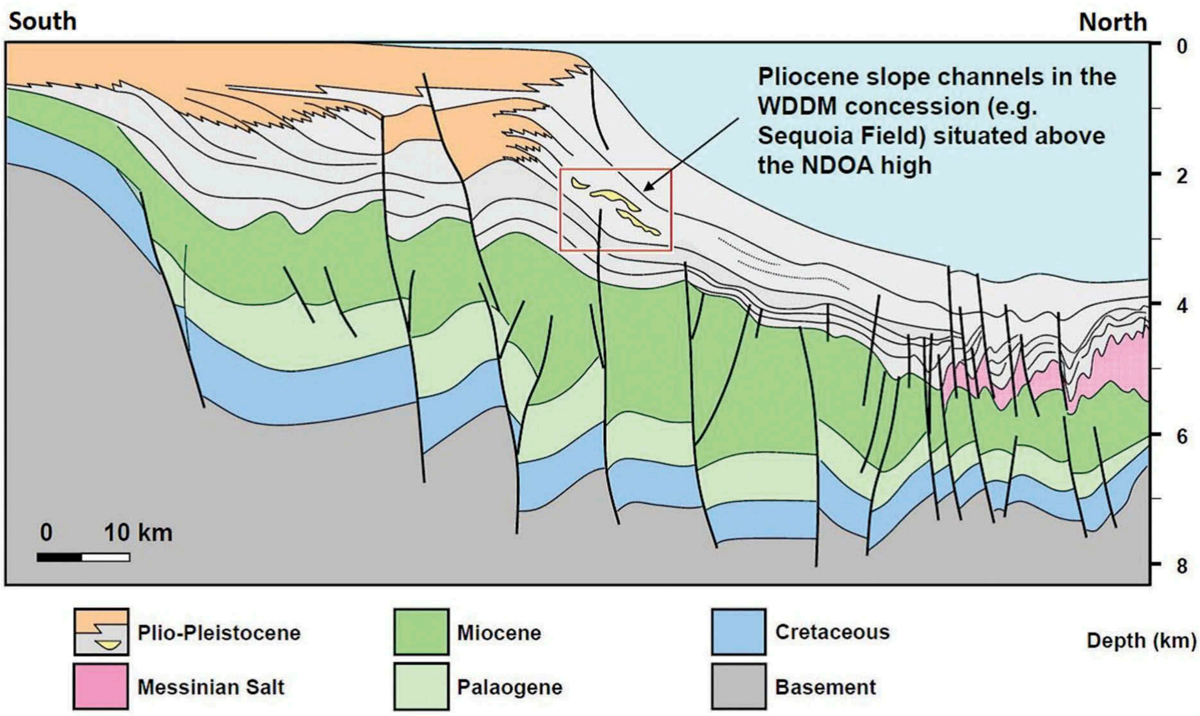

Figure 3. Nile Delta Tectono-Stratigraphic setting (Cross et al. 2009).

main aim of this study, to determine the reservoir quality in Sequoia Field.

3. Materials and methods

The petroleum potential of Late Pliocene El Wastani Formation clastic reservoir rock in the study area was evaluated using five wells (Sequoia-D1, Sequoia-D3, Sequoia-D5, Sapphire-1, Sapphire-2). The basis for petroleum potential evaluation is the petrophysical analysis of targeted intervals in all wells. This includes lithology interpretation gained from cross-plots, contouring various petrophysical properties, and outlining the vertical distribution of petrophysical properties.

3.1. Shale volume determination

Shale volume (V_{sh}) is very important because it helps to discriminate between reservoir and non-reservoir rock (Schlumberger 1984).The following equation is used to determine the shale volume:

$$I_{GR} = \frac{GR_{log} - GR_{min}}{GR_{max} - GR_{min}} \quad (1)$$

where I_{GR} = Gamma ray index, that can be corrected to V_{sh} using Dresser Atlas chart (Atlas 1979).

GR_{log} = gamma ray reading of formation;

GR_{min} = minimum gamma ray; GR_{max} = maximum gamma ray

3.2. Determinations of formation porosities (ø)

Porosity is the ratio of void space in a rock to the total volume of rock, and reflects the fluid storage capacity of the reservoir. Total porosity can be easily determined using sonic, density and neutron logs (Schlumberger 1984).

3.3. Determination of fluid saturation

Determination of the fluid saturation means principally the differentiation between the various types of fluid components (water and hydrocarbons). The hydrocarbons, in turn, need the separation between the movable and residual types (Schlumberger 1984).

Water saturation S_w is the most important petrophysical parameter used for the evaluation of a certain reservoir (Schlumberger 1984). Water saturation is calculated using different equations of which Archie's Indonesian is the most important.

$$\frac{1}{\sqrt{R_t}} = \left(\sqrt{\frac{\phi^m}{aR_w}} + \frac{V_{cl}^{\left(1 - V_{cl/2}\right)}}{\sqrt{R_{cl}}} \right) S_w^{n/2} \quad (2)$$

where; R_{sh}: is the resistivity of a thick shale unit, R_t: is the true resistivity of the uninvaded zone,

4. Results and discussions

4.1. Lithological identification cross-plots

Identification of lithology is of a particular importance in the formation evaluation process. Logs can be used as indicators of lithology. The most useful logs for this purpose are density, neutron, sonic and gamma-ray logs. Figure (4) shows the neutron density cross-plot (lithological identification cross plot) of El Wastani Formation in all wells. As is shown in this Figure major of the plotted points are scattered and lying on sandstone line. Minor points are lying between sandstone and limestone lines for the small values. The deviation of the scattered points away from the sandstone line may be clarified by the presence of clay minerals and calcareous cementation, while the deviation of minor points towards dolomite line is related to fine-grain sandstone, based on the distribution of points, this indicates the presence of gas in the area where the five wells still production from this area.

4.2. Vertical variations of petrophysical characteristics

The vertical distribution of hydrocarbon occurrence can be clarified and presented through the construction of the litho-saturation cross-plots (CPI) (El-Khadragy et al. 2017).

Figure (5) demonstrates the computer processed interpretation (CPI) plot for the El Wastani Formation Sequoia channel in Sequoia-D1well. It is encountered at depth ranges from 1520 m to 1654 m. The gross interval is 132 m. It is exposed in this figure and characterised by the predominance of sandstone and Shale where the sandstone tends to increase in the north parts of the Formation. Depend on the lithofacies distribution of the studied formation. The effective porosity and the hydrocarbon saturation increase in the north parts of this formation while the shale volume and water saturation decrease towards this part (high-quality sandstone). In this well, the shale content is 22%, the effective porosity is 29%, the water saturation is 0.40%, and the net pay is 58 m. It is obvious that the facies effect is the main factor that is controlling the distribution of the petrophysical properties, within ElWastani sandstone Sequoia channel, in Sequoia-D1 well.

Figure (6) proves the computer processed interpretation (CPI) plot for El-Wastani Formation Sequoia channel in Sequoia-D3 well. It is encountered at depth ranges from 1447 m to 1530 m. The gross interval is 83 m. As exposed in this figure, it is mainly characterised by the predominance of sandstone and shale where the sandstone tends to increase in the lower parts of the Formation. Depending on the lithofacies distribution of the studied Formation, the effective

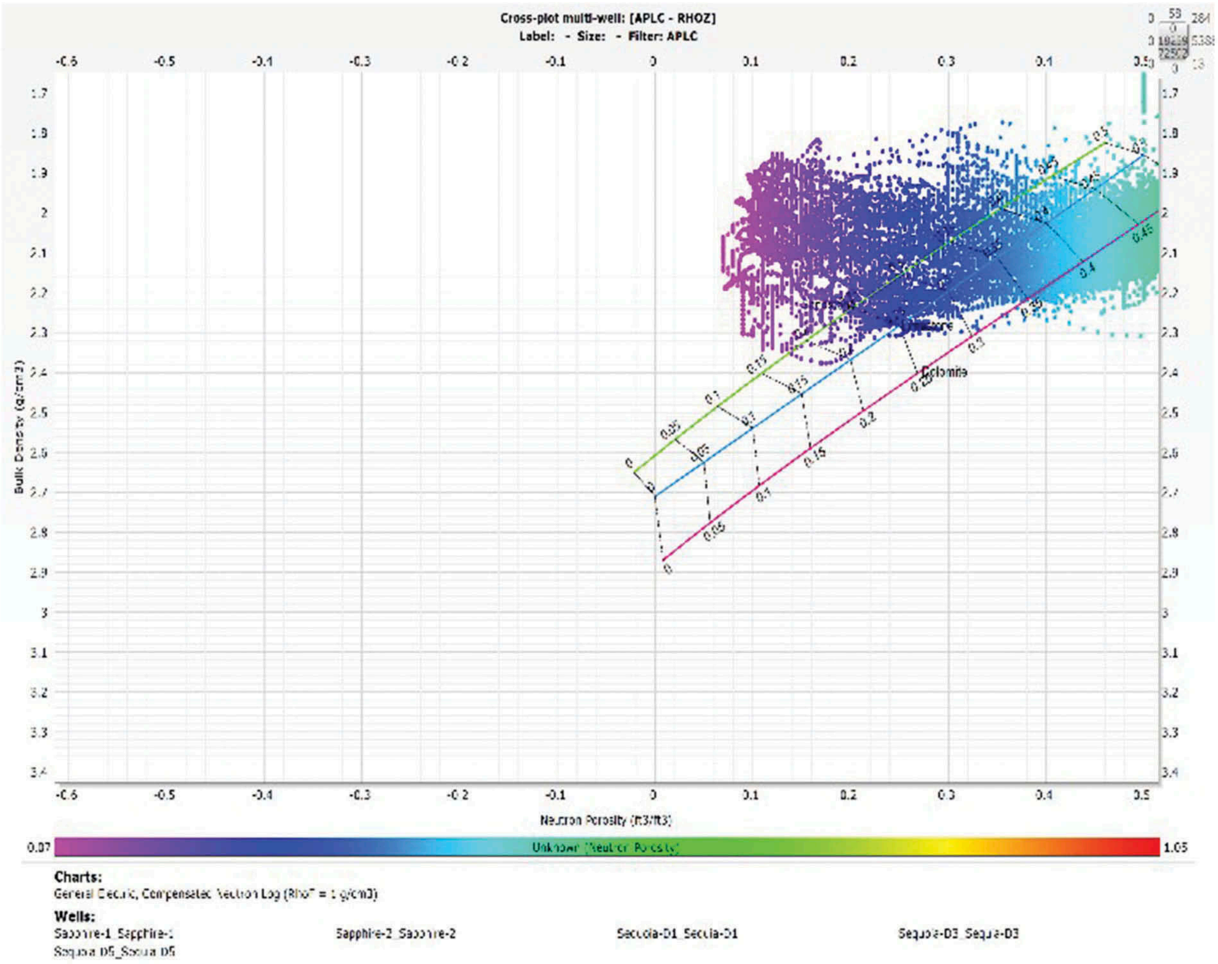

Figure 4. Multi well density to neutron cross plot of El Wastani Sequoia channel in the studied wells.

porosity and the hydrocarbon saturation increase in the lower parts of this Formation, while the shale volume and water saturation decrease towards these parts (high-quality sandstone). The shale content is 28%, the effective porosity is 25%, the water saturation is 26%, and the net pay thickness is 26 m. It is clear that the facies effect is the main factor that is controlling the distribution of the detected petrophysical properties, within El Wastani sandstone Sequoia channel, in Sequoia-D3 well.

Figure (7) explains the computer processed interpretation (CPI) plot for El Wastani Formation Sequoia channels in Sequoia-D5 well. It is encountered at depth ranges from 1450 m to 1627 m. The gross interval is 177 m. As it is shown in this Figure, it is mainly characterised by the predominance of sandstone and Shale where the sandstone tends to increase in the middle and lower parts of the Formation. Depending on the lithofacies distribution of the studied Formation, the effective porosity and the hydrocarbon saturation increase in the middle and lower parts, where shale volume and water saturation decrease towards these parts (high-quality sandstone). As it revealed in this figure, the shale content ranges about 29%. The effective porosity ranges about 20%. The water saturation ranges about 20%. The net pay ranges about 46 m. It is clear that the facies effect is the main factor that is controlling the distribution of the petrophysical properties, within El Wastani sandstone Sequoia channel, in Sequoia-D5 well.

Figure (8) explains the computer processed interpretation (CPI) plot for El Wastani Formation Sequoia channels in Sapphire-1 well. It is encountered at depth ranges from 1460 m to 1587 m. The gross interval is 127 m. As it is shown in this Figure, it is mainly characterised by the predominance of sandstone and Shale where the sandstone tends to increase in the middle and upper parts of the Formation. Depending on the lithofacies distribution of the studied Formation, the effective porosity and the hydrocarbon saturation increase in the middle and upper parts, where shale volume and water saturation decrease towards these parts (high-quality sandstone). As it revealed in this figure, the shale content ranges about 22%. The effective porosity ranges about 25%. The water saturation ranges about 17%. The net pay ranges about 10 m. It is clear that the facies effect is the main factor that is controlling the distribution of the petrophysical properties, within El Wastani sandstone Sequoia channel, in Sapphire-1 well.

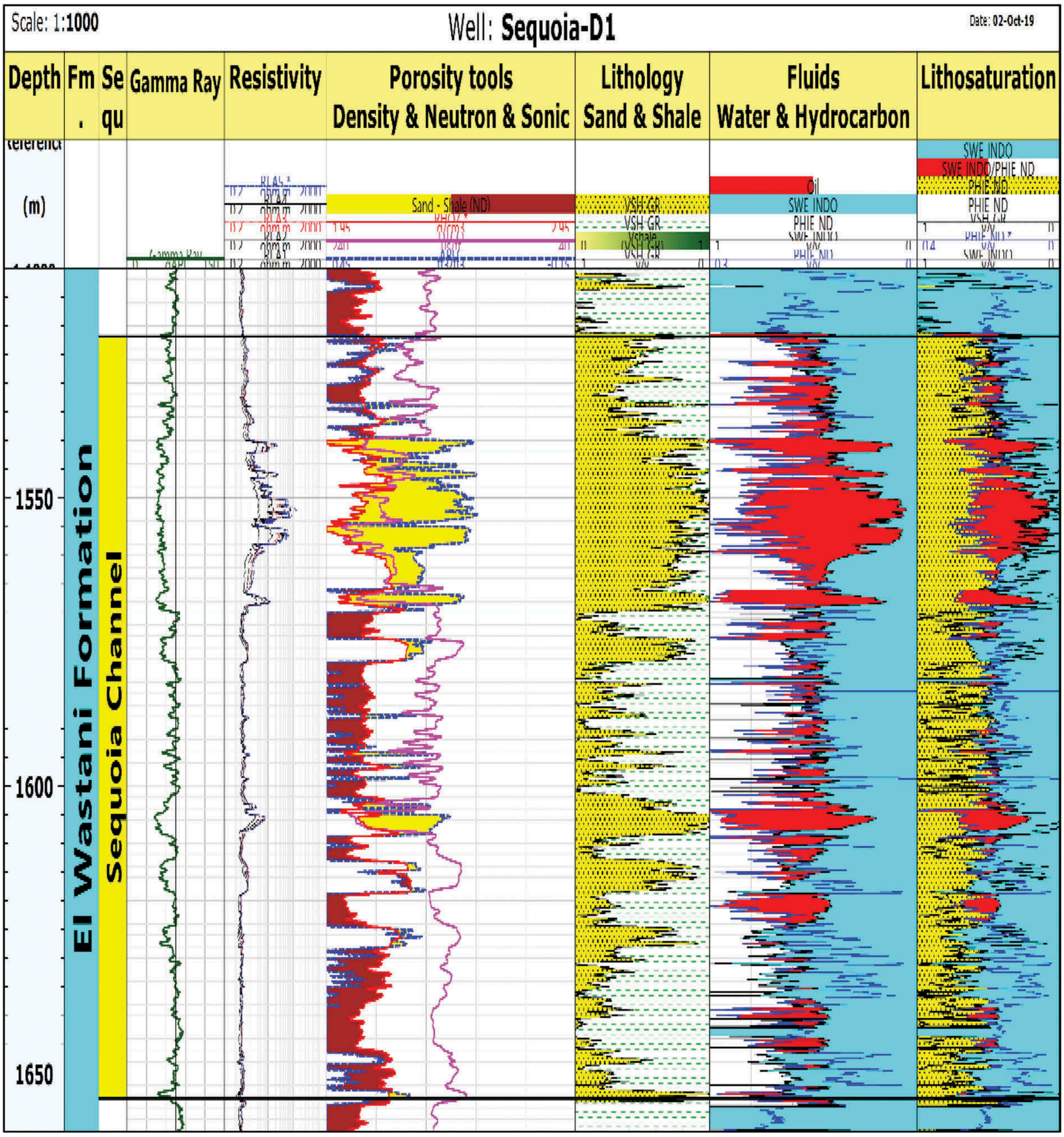

Figure 5. Litho-saturation cross-plot of El-Wastani formation Sequoia channel in Sequoia-D1 well.

Figure (9) explains the computer processed interpretation (CPI) plot for El Wastani Formation Sequoia channels in Sapphire-2 well. It is encountered at depth ranges from 1534 m to 1577 m. The gross interval is 43 m. As it is shown in this Figure, it is mainly characterised by the predominance of sandstone and Shale where the sandstone tends to increase in the middle and upper parts of the Formation. Depending on the lithofacies distribution of the studied Formation, the effective porosity and the hydrocarbon saturation increase in the middle and upper parts, where shale volume and water saturation decrease towards these parts (high-quality sandstone). As it revealed in this figure, the shale content ranges about 10%. The effective porosity ranges about 29%. The water saturation ranges about 15%. The net pay ranges about 24 m. It is clear that the facies effect is the main factor that is controlling the distribution of the petrophysical properties, within El Wastani sandstone Sequoia channel, in Sapphire-2 well.

4.3. Lateral variations of petrophysical characteristics

The reservoir properties of the Late Pliocene El Wastani Formation (Sequoia Channel) reservoirs extracted from well-logging data were averaged and shown in Table 1.

Figures (10 and 11) shows maps and histograms of the petrophysical properties within El Wastani Formation Sequoia Channel. All maps show an accurate matching between the measured

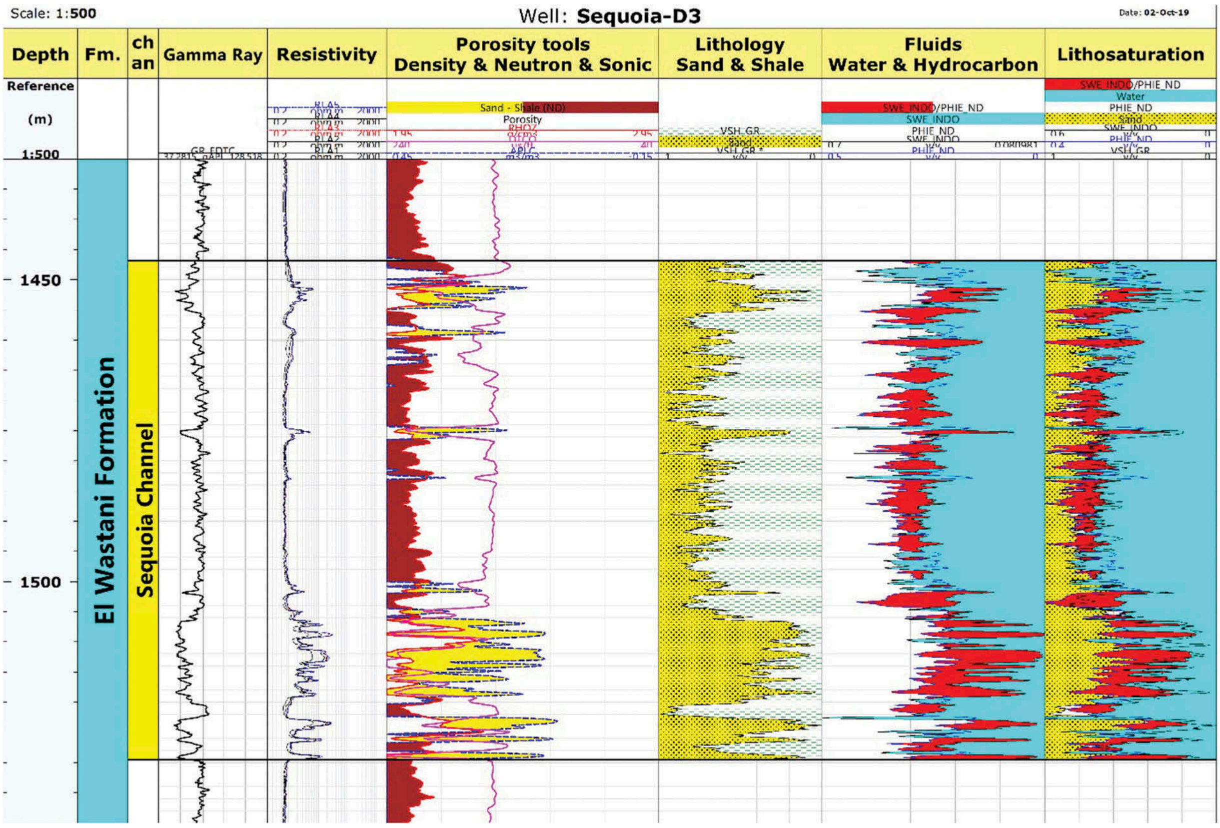

Figure 6. Litho-saturation cross-plot of El-Wastani formation Sequoia channel in Sequoia-D3 well.

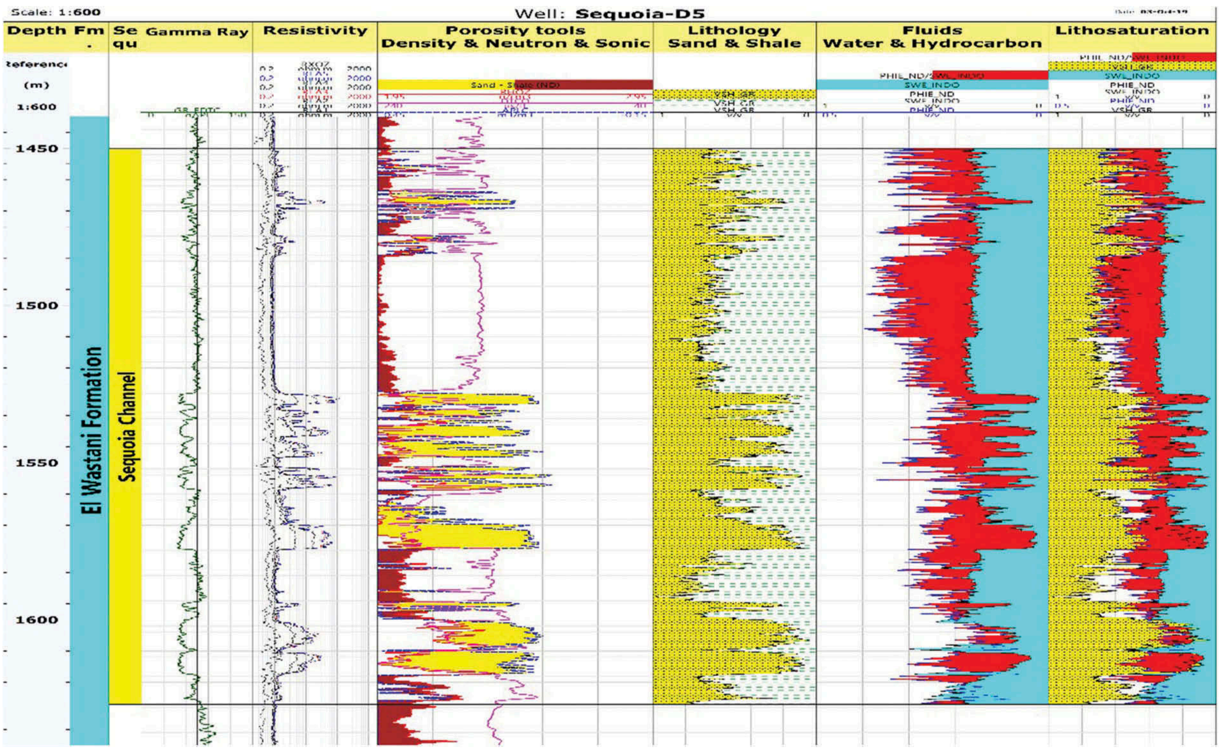

Figure 7. Litho-saturation cross-plot of El Wastani formation Sequoia channel in Sequoia-D5 well.

petrophysical properties. This distribution pattern indicates the hydrocarbon potential of the El Wastani Formation Sequoia Channel. The hydrocarbon saturation and effective porosity increase towards the NE parts while the shale volume and water saturation increase towards the

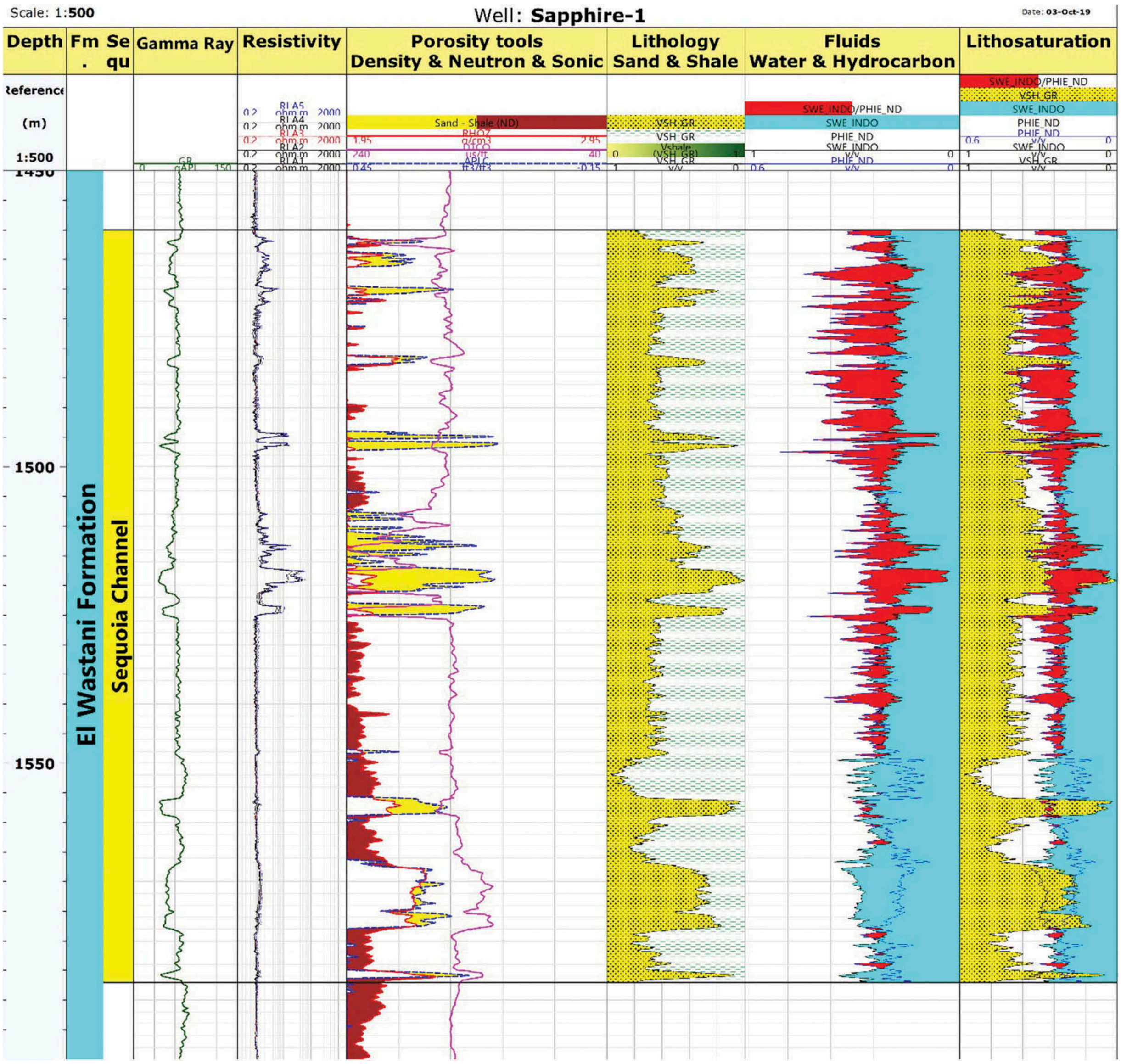

Figure 8. Litho-saturation cross-plot of El-Wastani formation Sequoia channel in Sapphire-1 well.

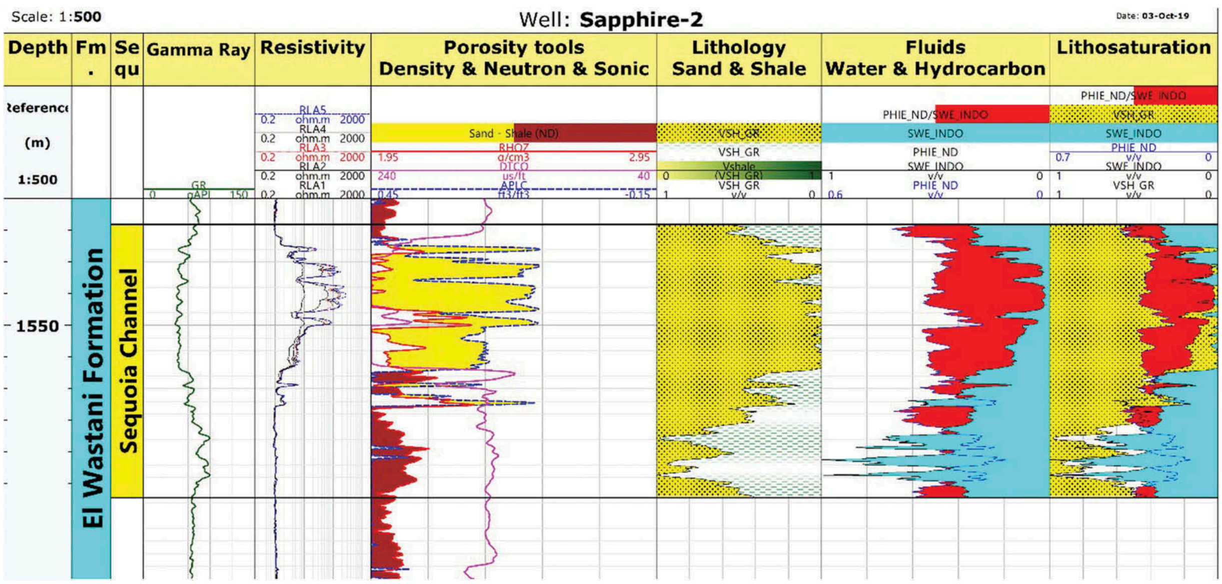

Figure 9. Litho-saturation cross-plot of El-Wastani formation Sequoia channel in Sapphire-2 well.

Table 1. Reservoir properties of El Wastani Sequoia channel contains a volume of Shale (V sh %), effective porosity (PHIE%), water saturation (Sw%), hydrocarbon saturation (Sh%), and the total producing from reservoir (Net Pay).

WELL	V sh(%)	PHIE(%)	Sw(%)	Sh(%)	Net Pay
Sequoia-D1	0.224	0.291	0.395	0.605	57.929
Sequoia-D3	0.283	0.25	0.257	0.743	25.773
Sequoia-D5	0.278	0.194	0.203	0.797	45.97
Sapphire-1	0.217	0.254	0.171	0.829	10.06
Sapphire-2	0.091	0.288	0.147	0.853	23.67

SW parts. As exposed in this figure. Sand thickness ranges between 10 m and 58 m in wells Sapphire-1 and Sequoia-D1, respectively. The effective porosity occurrences are observed within the range of 19% to 29%. The shale content is observed within the range of 10% to 28%. The water saturation is observed within the range of 15% to 40%. It is obvious that the facies effect is the main factor that is controlling the distribution of the petrophysical properties, within El Wastani sandstone Sequoia Channel in the study area.

5. Conclusions

Petrophysical properties derived from the conventional well logging analysis are generally diverse laterally in the form of iso-parametric maps and vertically in the form of lithosaturation cross plots. The Pliocene El Wastani Formation Sequoia Channel are mainly characterised by the predominance of sandstones and Shale. Analysis

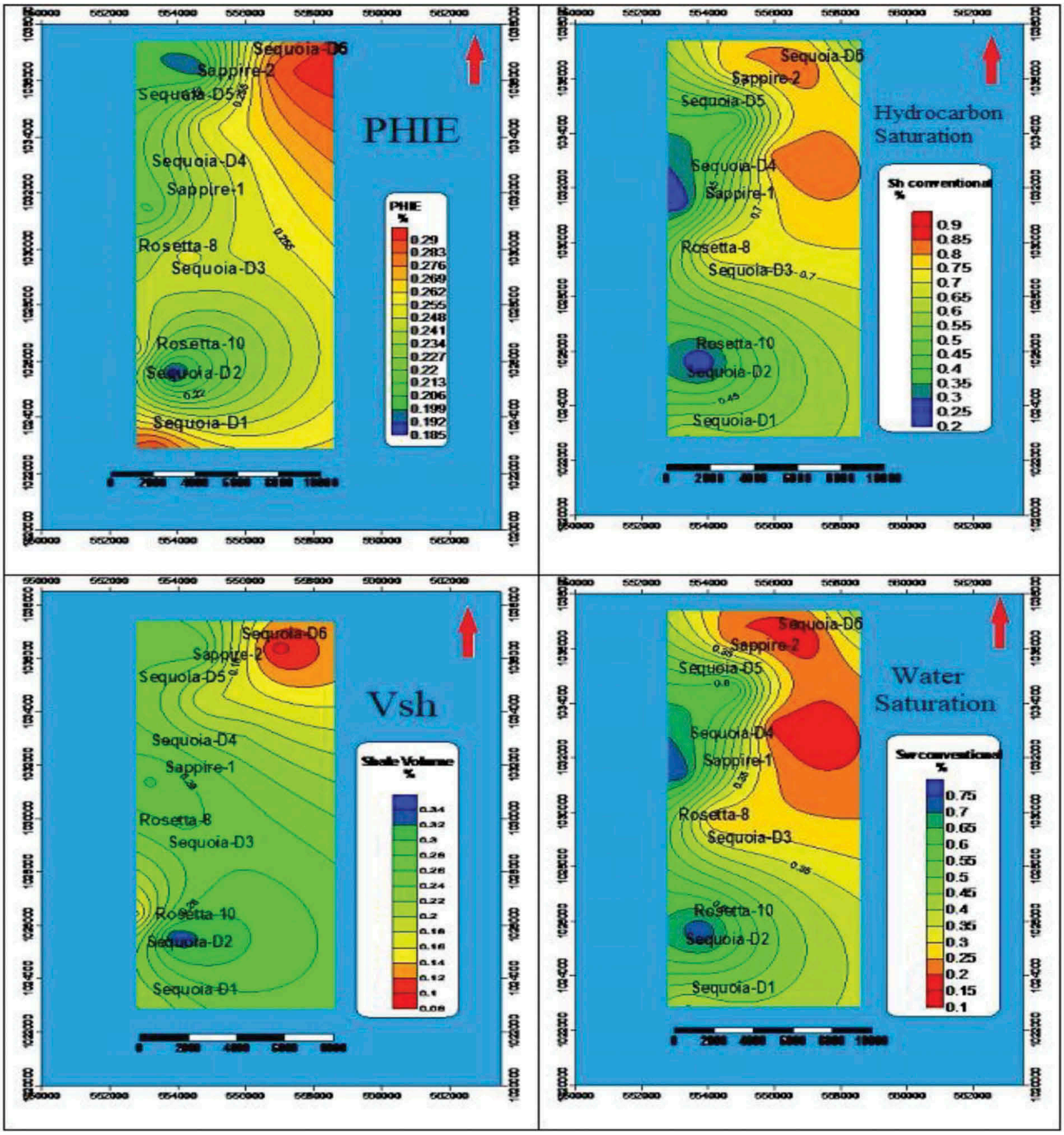

Figure 10. Petrophysical properties of El Wastani formation Sequoia channel.

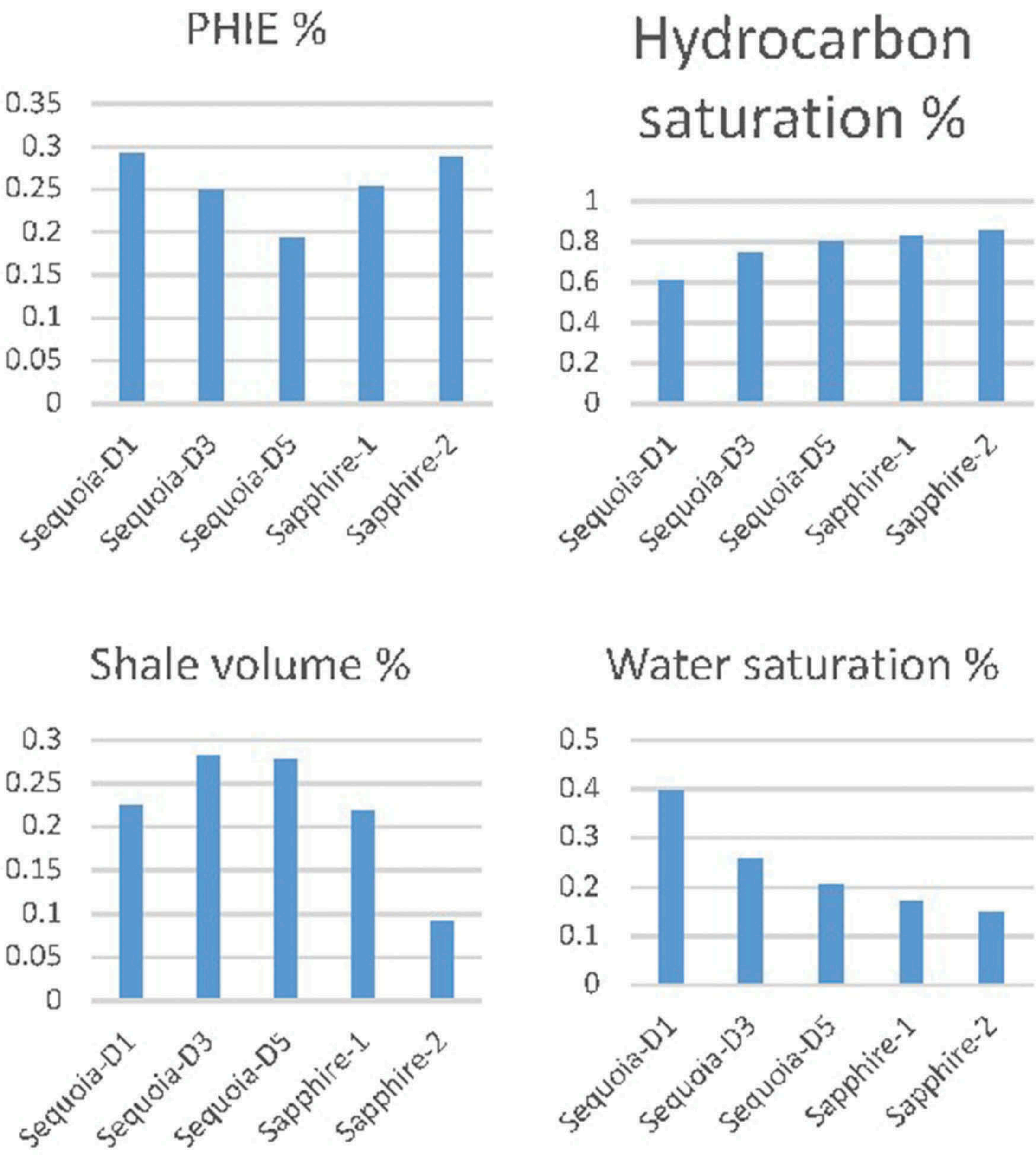

Figure 11. Graphical of the petrophysical properties of the El Wastani formation Sequoia Channel.

results in effective porosity ranges between 19% and 29%, shale content ranges between 10% and 28%, the water saturation ranges between 15% and 40%. Petrophysical investigation of Sequoia Channel of the Late Pliocene El Wastani Formation revealed the presence of significant petrophysical properties led to the better accumulation of clear quantity of hydrocarbons in Sequoia Field. According to the presented discussions, the Gas accumulation in Sequoia field does not only depend on the structural configuration of the field but also depend on the lithofacies distribution of the studied Formation. A new prospect area could be suggested in the north east corner of the study area where the effective porosity and the hydrocarbon saturation increase while the Shale content seems to be low (high-quality sandstone).

Acknowledgements

Authors express the gratitude to Egyptian General Petroleum Corporation, and to Rashid Petroleum Company, for providing data have been used in our study.

Disclosure statement

No potential conflict of interest was reported by the authors.

References

Abdel Aal A, El Barkooky A, Gerrits M, Meyer H, Schwander M, Zaki H. 2000. Tectonic evolution of the Eastern Mediterranean basin and its significance for hydrocarbon prospectivity in the ultradeepwater of the Nile Delta. The Leading Edge. 19(10):1086–1102.

Alami R. 2006. Egypt's domestic natural gas industry. Oxford (UK): Oxford Institute for Energy Studies.

Atlas D. 1979. Log interpretation charts: houston. Texas: Dresser Industries.

Cross NE, Cunningham A, Cook RJ, Taha A, Esmaie E, El-Swidan N. 2009. Three-dimensional seismic geomorphology of a deep-water slope-channel system: the Sequoia field, offshore west Nile Delta, Egypt. Am Assoc Pet Geol Bull. 93 (8):1063–1086.

Doherty M, Jamieson T, Kileni T, Trayner P (1988) The geology and seismic stratigraphy of the offshore Nile Delta. In: Ninth petroleum exploration and production conference, the Egyptian general petroleum corporation (EGPC), Cairo, Egypt (Vol. 2, p. 408–42).

El-Khadragy AA, Shazly TF, Ramadan M, El-Sawy MZ. 2017. Petrophysical investigations to both Rudeis and Kareem formations, Ras Ghara oil field, Gulf of Suez, Egypt. Egyptian Journal of Petroleum. 26(2):269–277.

Harms JC, Wray JL. 1990. Nile Delta. In: Said R, editor. Geology of Egypt. The Netherlands: AA Balkema; p. 329–343.

Mayall M, Jones E, Casey M. 2006. Turbidite channel reservoirs—key elements in facies prediction and effective development. Marine and Petroleum Geology. 23(8):821–841.

Mayall M, Stewart I. (2000 Dec). The architecture of turbidite slope channels. In: Deep-water reservoirs of the world: SEPM, Gulf coast section, 20th annual research conference (Vol. 578, p. 586). Houston: GCSSEPM Foundation.

Mohamed IA, El-mowafy HZ, Fathy M. 2015. Prediction of elastic properties using seismic prestack inversion and neural network analysis. Interpretation@SEG & AAPG. 3(2):57–68.

Samuel A, Kneller B, Raslan S, Sharp A, Parsons C. 2003. Prolific deep-marine slope channels of the Nile Delta, Egypt. AAPG Bull. 87(4):541–560.

Schlumberger. 1984. Well evaluation conference. Egypt: chapter 1 geology of Egypt. Cairo (Egypt): Schlumberger Middle East.

Vandré C, Cramer B, Gerling P, Winsemann J. 2007. Natural gas formation in the western Nile delta (Eastern Mediterranean): thermogenic versus microbial. Org Geochem. 38(4):523–539. doi:10.1016/j.orggeochem.2006.12.006

Younes M. 2001. Reservoir characterization and hydrocarbon potential habitat in the Abu Qir gas field, offshore Nile Delta, Egypt. Proceedings of 5th Conference on Geochemistry, Alexandria University, Alexandria, Egypt (Vol. 2, p. 303–324).